Tribological characterization of the additively manufactured 18Ni300 maraging steel

João Coelho

joaommmvcoelho@tecnico.ulisboa.pt

Instituto Superior Técnico, Universidade de Lisboa, Portugal.

January 2021

Abstract

The growing need for better performance and more complex geometries has led to the appearance of new high resistance engineering materials, such as the maraging steel, which can inclusively be additively manufactured. However, few studies about its mechanical and tribological behavior exist in the literature. This study, then, presents a tribology study on 18Ni300 maraging steel using ring compression tests. Experimental tests were performed on conventional and additively manufactured maraging specimens, to compare the performance of both metallurgical conditions. The tests were carried out at different temperatures and strain rates, to better understand the effect of real metal shaping and cutting operations conditions on the friction coefficient. The ring compression tests shown a significant variation of the friction coefficient with temperature and speed (>50%). However, the manufacturing process of the specimens didn't have such a significant influence on the friction coefficient.

Keywords: *Ring compression, maraging steel, temperature, strain rate, friction*

1. Introduction

In recent years, metal shaping operations and new manufacturing technologies have been developed, as a consequence of the rising needs for better components with higher performance and more complex geometries. Consequently, new high resistance and high-performance engineering materials have been emerging in the last decades, known for their high temperature resistance, high corrosion resistance or high strength to weight ratio. When studying a new material, mechanical resistance, plasticity and microstructural aspects are some of the most analyzed factors. Another important aspect is the quantification of friction, as a performance indicator of mechanical components and determinant factor to reduce energy and wear, despite the lack of studies regarding its analysis present on the literature. This fact, combined to the little knowledge about these new engineering materials, motivates the present study, which focus on the friction coefficient's variation with temperature, speed and metallurgical condition (conventional vs. additively manufactured) on the maraging steel – conventional and additively manufactured.

Maraging steels are known for their superior strength and toughness without much ductility compromise, due to the precipitation of inter-metallic compounds (Bhukya, *et al*, 2014). In addition, ageing treatment (>480ºC) can modify phase composition, promote austenite reversion and/or increase intermetallic precipitation, as found by Lohman et al 2019. The extent of these phenomena depends on the time and temperature of the heat treatment. The excellent mechanical properties allied to a good weldability, promoted by the lack of carbon, make grade 300 maraging a very suitable material for additive manufacturing (Turk et al. 2019). The higher mechanical strength of the additively manufactured grade 300 maraging, when compared with its conventional counterpart, is due to the strong thermal gradients of the SLM process, that promote a fine-grain microstructure. In addition, the typical columnar microstructural grain geometry, aligned with build direction, results in a higher number of grain boundaries in the perpendicular direction, leading to an anisotropic behavior of these materials with an increased strength performance when loaded in a perpendicular direction to build (Prashanth and Eckert 2017). The reverted austenite is reported to increase the materials' ductility due to its transformation into martensite, (transformation induced plasticity) which additionally enhances the strength-ductility ratio of maraging steels (Bajaj 2020). Regarding friction characterization, it is reported that it significantly varies with ageing condition (time and temperature) for the additively manufactured maraging (S, Yin et al. 2018). There is, however, a lack of studies that focus on tribological characterization.

Consequently, the present work aims at providing a friction analysis of the maraging steel under high speed and temperature conditions, to portray realistic

operating conditions of high strength engineering materials. Regarding the tribological characterization, one of the most widely accepted way to evaluate the tribological behavior of a given material is performing ring compression tests. This test consists of compressing a ring-shaped specimen and measuring its change in height and internal diameter throughout the process, using different tribological conditions (i.e., dry or lubricated). Its simplicity comes from the fact that friction coefficient (μ) can be evaluated only by measuring the changes in the shape of the specimen. The more deformation the material suffers, the higher the coefficient of friction (Male, 1965). On the present work, the roughness of the compression plates is practically zero, enhancing the friction adhesion mechanism and minimizing others, such as the interlocking, thus promoting a more accurate study. Adhesion is still one of the most complex phenomena to investigators that occur on solid-solid clean interfaces, being mainly activated with lower roughness values. Some suggest that covalent, ionic and metallic bonds are the microscopic causes, being more prevalent than the weaker hydrogen and van der Waals bonds (Bhushan, 2003). The author additionally suggests an increase of friction by adhesion with temperature.

Later, some authors started studying the effects of temperature changes in the ring compression test. Shahriari et al. (2011) found an increase on the friction coefficient with temperature (1175ºC and 1100ºC) when conducting ring compression tests on Nimonic 115 superalloy using different lubricating conditions. The authors still state that the hot ring compression test (ring compression test performed at high temperatures) is a good way to estimate the flow stress behavior and performance of a lubricant.

Other factor that has driven some attention from investigators is the strain rate effect on the ring compression test. Male (1965) suggests that an increase in the press speed can provide greater lubrication efficiency when using soft or liquid lubricants. Garmong et al. (1977) also states that strain rate sensitive materials are more likely to changes in the friction coefficient when using different test speeds. Other authors (Börder, 2005, Asai, et al., 2017) studied the combined effects of temperature and strain-rate on the coefficient of friction. Börder (2005) studied the relative influence of these parameters on the ring compression test using steel specimens and polished compression platens, concluding that temperature is the most influential factor, followed by tool coating, and finally, speed (strain rate). Asai et al. performed high temperature (1100 ºC) and speed (50 $mm.s^{-1}$) ring compression tests and reported a slight change in the coefficient of friction under those conditions.

However, given the novelty of this material, there are few studies regarding its tribological behavior at high temperatures, and specially, at high strain rates (>5000 s^{-1}), which is important towards an improved understanding and assessment, thus enabling the process optimization on this given material. Some authors (Sun, 2020, Opalinski, 2016) used the pin-on-disc test on this material, suggesting that abrasion is the main wear mechanism (Sun, 2020), but very few studies regarding ring compression tests on the maraging steel exist.

In short, the present work intends to tackle the following questions:

- How is the coefficient of friction affected by temperature?
- How is the coefficient of friction affected by strain rate?
- How is the coefficient of friction affected by the manufacturing process of a given material?
- How will the maraging steel's friction coefficient vary under these conditions?
- What of these parameters is the most influential to the coefficient of friction?

2. Proposed numerical-experimental procedure

The identification of the friction coefficient was conducted through a comparison of the ring compression experimental results with numerically-built calibrated curves for distinct levels of friction. This comparison is conducted for each tested temperature and strain rate conditions in dry friction conditions.

2.1. Identification of the frictionless flow stress

In order to build the calibrated curves, it is necessary to find the materials flow stress, for each temperature and strain-rate tested condition. Such was performed through the compression of cylindrical specimens (⌀ 4 x 4mm). Despite using graphite as lubricant in order to

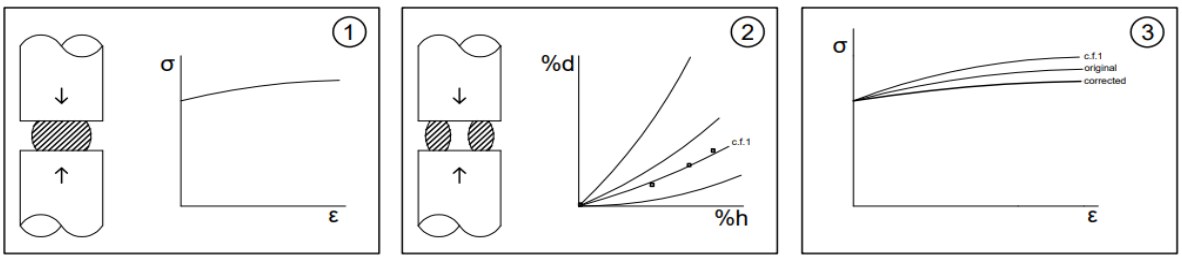

Figure 1 - Flowchart explaining the process used to obtain the stress-strain curves corresponding to frictionless conditions

minimize friction, the obtained strain-stress curve includes is not frictionless. Figure 1 illustrates the procedure for obtaining the frictionless flow stress. Firstly, compression tests for all combinations of strain-rate and temperature were performed under lubricated conditions, enabling the identification of a preliminary flow stress represented as "original" in figure 1-1. Secondly, ring compression tests were performed for the exact same conditions of the cylindrical compression tests and preliminary calibration curves were numerically obtained using the preliminary flow stress, allowing for the identification of the friction coefficient (c.f.1) of the ring test, as shown in figure 1-2. Finally, the cylindrical compression test was numerically simulated inputting the obtained friction coefficient and enabling the correction of the strain-stress, through subtraction of the friction overestimation of the c.f.1 curve. The corrected (frictionless) stress-strain curve is thus obtained, as illustrated in figure 1-3.

2.2. Friction identification for distinct temperature and strain-rate conditions

The final calibrated curves were obtained numerically (commercial FEA software), using the frictionless flow stress curve as the material input. In order to decrease the computational cost, only one quarter of the operation was considered, as represented in figure 2. The ring dimensions are the same as the ones used in the determination of frictionless flow stress (outer diameter of 8 mm, inner diameter of 4 mm, height of 3 mm). A mesh composed of 3350 axisymmetric elements with reduced integration was used for the ring compression simulations, and 2500 elements for the uniaxial compression simulations.

A new set of ring compression tests were performed for a wide range of temperatures and strain-rates, in dry condition, enabling the identification of the friction coefficient in function of the tested (strain-rate and temperature) conditions for both additively and conventionally manufactured grade 300 maraging.

3. Experimental methods

In this section, the experimental methods used to perform the ring compression tests will be presented. In the first subsection, the experimental setup used in the ring compression tests will be detailed. The plan of ring compression experiments carried is shown in the second subsection.

3.1. Experimental setup

The ring compression tests were performed on a customized split-Hopkinson pressure bar (SHPB), which can provide a wide range of strain-rate conditions, as show in figure 3. The main components are an impact bench, a pneumatic gun (to provide the necessary power for the high-speed tests) and a hydraulic ram cylinder (to perform the low-speed tests). The impact bench is composed of basic structural parts and two compression platens made of WC-Co, with a nano composed PVD coating, HiPIMS of TiAlSiN technology and 3 thickness micrometers (provided by Palbit, SA). The compression platens used in the experimental tests have been machined and polished to limit surface temperatures, a furnace was used (which can go up to 400ºC). The inner diameter, outer diameter and height of the ring-shaped specimens were measured before, during and after the experiments using a digital Vernier

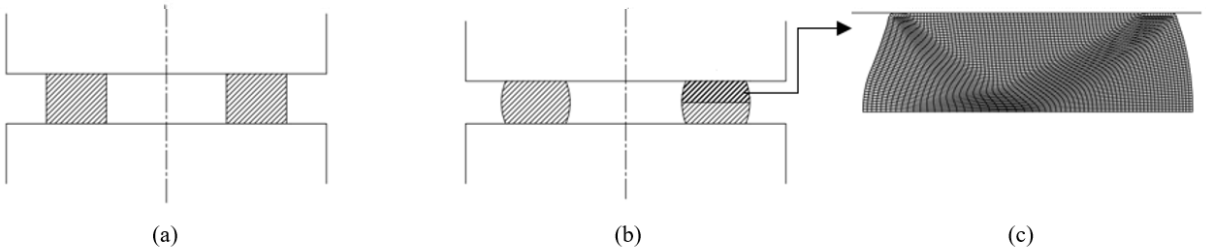

Figure 2 – Finite elements model of the ring compression test: (a) Scheme of the non-deformed specimen; (b) Scheme of the

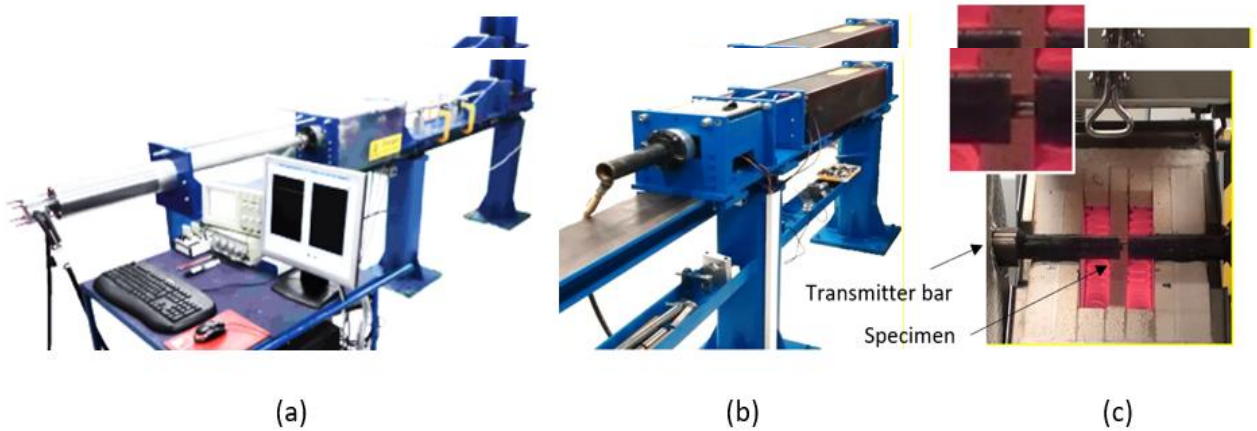

Figure 3 - Split-Hopkinson pressure bar that was utilized in the ring compression tests; (a) Configuration using the pneumatic actuator; (b) Using the hydraulic actuator; (c) Compression platens

caliper. A microscope was also used to confirm these values, using diascopic illumination.

3.2. Plan of experiments

As described in section 2, before performing dry ring compression tests, lubricated ring compression tests were carried to correct the σ-ε curves (step 2 of figure 1). Three different lubricated ring compression tests were carried in the three most "extreme" combined strain rate-temperature conditions: quasi-static (QS) at room temperature (RT – approximately 25ºC), QS at 400ºC, 6000 s^{-1} at 400ºC. These experiments are shown below in tables 1 and 2 ("Lub").

v/T	25ºC	200ºC	400ºC
Q.S.	Dry + Lub	Dry	Dry + Lub
V1	Dry	Dry	Dry
V2	Dry	Dry	Dry + Lub

Table 1 – Plan of experiments for the conventional maraging specimens

v/T	25ºC	200ºC	400ºC
Q.S.	Dry + Lub	Dry	Dry + Lub
V2	Dry	Dry	Dry + Lub

Table 2 – Plan of experiments for the AM maraging specimens

Having the final frictionless σ-ε curves, the dry experiments on maraging steel specimens (both wrought and additively manufactured) were carried at RT, 200ºC and 400ºC, and using three different strain rates: QS, 300 s^{-1} (V1) and 6000 s^{-1} (V2).
Due to the high cost per Kg of AM maraging, only two different strain rates were tested (the lowest one, QS, and the highest one, 6000 s^{-1}).

4. Results and discussion

The results of the present work are divided into three subsections. In the first subsection, the corrected curves resultant from the procedure described in the previous section are shown. In the second subsection, the final calibration curves are represented simultaneously with the dry ring compression experimental results. Finally, in the last subsection, the friction coefficients obtained are shown, as well as their variation with temperature, test speed and metallurgical condition.

4.1. Corrected σ-ε curves

Two of the frictionless curves obtained from applying the procedure described in figure 1 are represented below in figure 4.

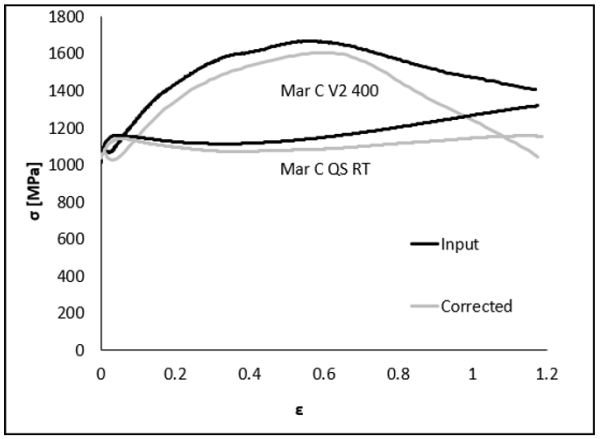

Figure 4 – Original and frictionless curves for conventional maraging at 6000 s^{-1} (V2) and 400ºC conditions, corrected with μ = 0.13, and at quasi-static (QS) and 25ºC (RT) conditions, corrected with μ = 0.09

As shown in figure 4, the original σ-ε curves have, not only different aspects, but also different strain hardening exponents (the more temperature and strain rate, the more positive the strain hardening exponent). Besides, as expected, the bigger the coefficient of friction used to correct the σ-ε curve, the bigger the distance between the original and the corrected curve, as represented in figure 4.

4.2. Ring compression tests

The friction coefficient values between the WC – maraging steel interface were determined by comparing the calibration curves with the experimental results. Two of these calibration curves (corresponding to QS 200ºC and V2 200ºC conditions) are shown in figure 5 below.

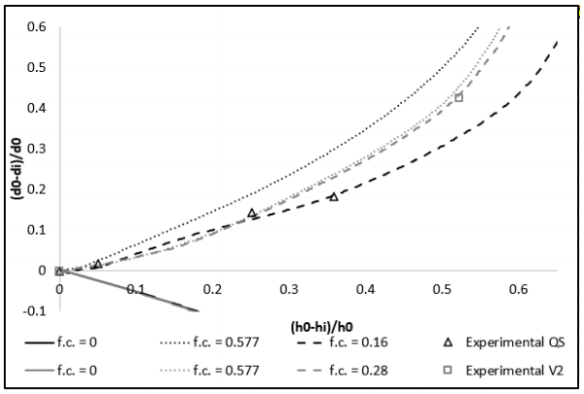

Figure 5 – Calibration curves and experimental results of ring compression tests for wrought maraging specimens at 200ºC and two different strain rates: QS and 6000 s^{-1} (V2)

The fact that for temperatures around 400ºC, the maraging steel can significantly increase its mechanical strength due to heat treatment, as suggested by Lohmann et al 2019, is consistent with the obtained results for those conditions: a maximum 10% height reduction in ring compression tests.

Relatively to the calibration curves, two phenomena were observed: the calibration curves are affected by the inserted σ-ε curve (as shown in figure 5, the curves corresponding to a friction coefficient of 0.577 are different), and in the high-speed σ-ε curves, the difference between the calibration curves corresponding to a higher friction coefficient (> 0.2) is smaller than in the quasi-static ones, as represented in the calibration curves of V2 200 maraging in figure 5. This last aspect made higher friction coefficient values harder to obtain accurately on high-speed experiments.

4.3. Friction coefficient variation with temperature, speed and metallurgical condition

The chosen low roughness of the compression platens minimizes plowing and interlocking friction effects and promotes friction by adhesion, which in turn allows for a more precise analysis and conclusions on friction values for the chosen interface.

The resulting friction coefficient values in function of temperature, strain rate and metallurgical condition are presented in figures 6 and 7 below (both dry and lubricated experiments – used to correct the σ-ε curves). As presented in these figures, excluding a few exceptions (the 25ºC tests for both AM and wrought maraging), the friction coefficient if higher in the dry tests than in the lubricated tests, which suggests that

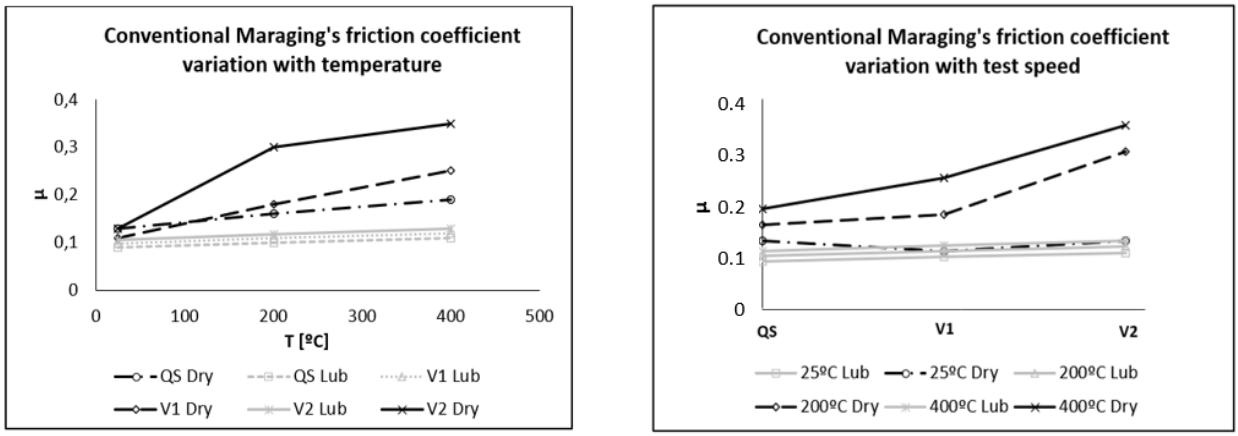

Figure 6 – Friction coefficient results for wrought maraging specimens shown in a graph of μ vs (a) Temperature; (b) Test speed

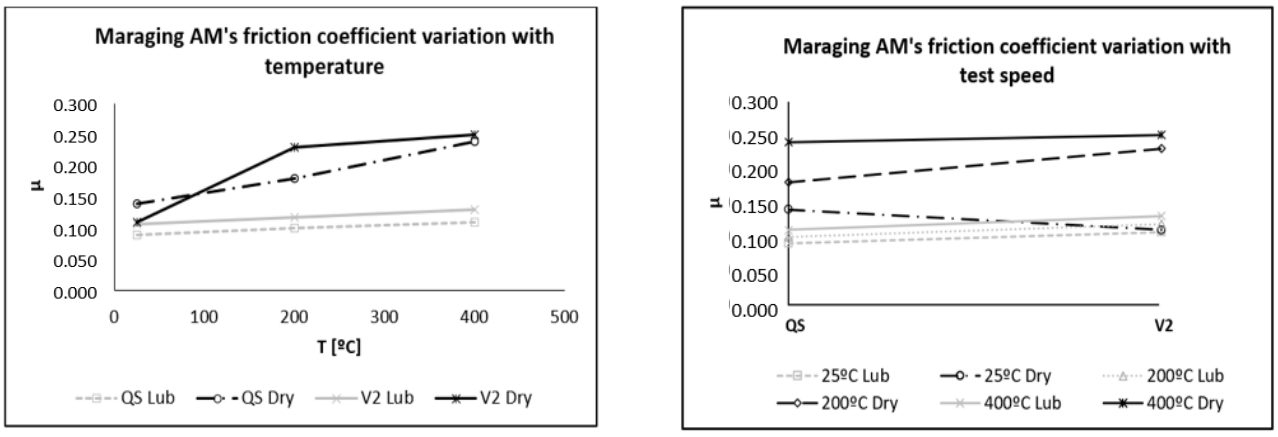

Figure 7 – Friction coefficient results for AM maraging specimens shown in a graph of μ vs (a) Temperature; (b) Test speed

the use of graphite as lubricant on a maraging – WC-Co interface reduces friction significantly, even at higher temperatures and strain rates, indicating that two lubricated surfaces with low roughness have a decrease on adhesion phenomena. This same result is proposed by Bhushan (2003). However, the friction on lubricated tests become slightly higher, the higher the temperature and test speed, which suggests lubricant degradation starts to occur.

On the dry experiments, the higher the test temperature, the higher the friction coefficient in both metallurgical conditions (wrought and additively manufactured material), with variations sometimes surpassing 50%. This same result is suggested by Bhushan (2003) when adhesion is the main friction mechanism present on a solid-solid interface. However, in both AM and wrought specimens, there is a lower difference between the friction coefficients at 200ºC and 400ºC, for a strain rate of 6000 s^{-1} (V2) – variations inferior to 20%.

The friction coefficient also tends to vary with test speed: for wrought maraging, it clearly increases with test speed for higher temperatures (200ºC and 400ºC), which is the opposite result obtained by Sun (2020), who performed pin-on-disc tests on maraging specimens. Strain rate is found to be a more influential factor on the friction coefficient than temperature on the present study, which is also in contrast with the results found by Börder (2005) on steel specimens. However, for AM maraging, the friction coefficient's variation with speed becomes inconclusive, as it decreases with speed at room temperature tests, increases at 200ºC, and is approximately constant at 400ºC. Combined higher temperatures and test speeds also seem to produce higher friction coefficients (variations superior to 50% at V2), in both materials.

On the other hand, the metallurgical condition doesn't seem to have an influence on the identified friction tendencies and values, in function of strain rate and temperature.

However, by analyzing some of the experimental measurements, the friction coefficient varies along the compression, as shown in figure 8.

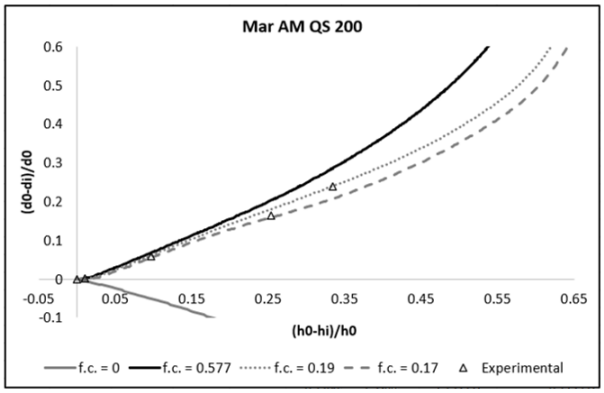

Figure 8 - Variation of the friction coefficient along the ring compression test

A quasi-static experiment was used to support this fact, as more accurate measurements are possible during this type of test. This reduction of the coefficient of friction is most certainly due to the oxides present on the specimen's surface, that disappear during the experiment, thus increasing the coefficient of friction along the process (the adhesion between a metal-ceramic interface is superior to the adhesion between an oxide-ceramic interface). This phenomenon has already caught the attention of some investigators, such as Cristino (2007). The author uses an argon-rich atmosphere successfully in order to reduce its initial percentage on the test interface, thus allowing the obtention of friction coefficient values exclusively of a solid-solid interface.

To complement figure 5-9, that demonstrates the friction coefficient reduction during the process due to the percentage of oxide present on the specimen's surface along the process, the friction coefficients of the oxide-ceramic and metal-ceramic interfaces will be estimated. In order to proceed with the calculations, the percentage of oxide and pure metal present in the surface need to be obtained. For that purpose, assuming that initially the surface is 100% oxide, and the percentage of oxide present will decrease with the area expansion during the process, the following formulas are proposed:

$$O = \frac{A_i}{A_f} \quad (1)$$

$$P = 1 - O \quad (2)$$

Where A_f is the area of the ring specimen's surface at the end of the experiment, A_i is the area of the specimen before the compression test, O is the percentage of oxide present on the surface at the end of the compression, and P is the percentage of pure metal at the end of the process. The estimation of the friction coefficient is then obtained by:

$$\mu = P.\mu_M + O.\mu_O \quad (3)$$

Where μ_M and μ_O are the friction coefficient of the metal-ceramic and oxide-ceramic interfaces, respectively. Using the experiment represented in figure 5-9, the following values can be obtained:

$$\begin{cases} O_{initial} = 1.0 \\ P_{initial} = 0.0 \\ O_{end} = 0.340 \\ P_{end} = 0.659 \end{cases}$$

Thus, knowing from figure 5-9 that $\mu_{initial} = 0.17$ and $\mu_{end} = 0.19$ using (28) at the beginning and at the end of the process with these values, we obtain:

$$\begin{cases} \mu_O = 0.17 \\ \mu_M = 0.229 \end{cases}$$

Therefore, demonstrating a significant difference between the friction coefficients present on metal-ceramic and oxide-ceramic surfaces, which suggests a variation of the friction coefficient during a ring compression experiment.

5. Conclusions

Due to the lack of tribological behavior characterization found in literature, this study pretended to provide more information about the friction coefficient's variation with important service parameters, such as temperature, strain rate and metallurgical condition of a new engineering material (18Ni300 maraging steel).
Thus, answering the questions presented on the introduction, the used combined approach between ring compression tests and the FEA software disclosed that the coefficient of friction tends to be higher, the higher the temperature and the test speed. The metallurgical condition (wrought vs AM maraging) didn't have a significant influence on the measured values. The chosen roughness of the compression platens used was practically zero, in order only have one phenomenon present, thus allowing more precise conclusions. Still, some variations of the friction coefficient along the process were found, and the presence of oxides on the surface of the material tends to be the main cause, as no controlled atmosphere was used.
Another conclusion that can be taken is the fact that there are no significant performance differences between AM and wrought maraging. The higher cost per Kg of AM maraging reflects on more complex attainable geometries without losing mechanical strength and tribological performance under extreme conditions.
This overall investigation intends to raise awareness to the fact that the tribological conditions may be affected by service conditions (i.e., temperature and strain rate), particularly, in new engineering materials with few studies and general mechanical knowledge and characterization, such as the maraging steel. Future works including higher roughness compression platens, allowing then asperities plastic deformation and other contributions to the friction coefficient are also suggested.

References

Ansell, T., Ricks, J., Park, C., Tipper, C., & Luhrs, C. (2020). Mechanical Properties of 3D-Printed Maraging Steel Induced by Environmental Exposure. *Metals*, *10*(2), 218.

Asai, K., Kitamura, K., Yukawa, N., & Hayashi, N. (2017). Estimation of friction by using improved calibration curves of ring compression test for hot forging of steel. *Procedia Engineering*, *207*, 2280-2285.

Bajaj, P., Hariharan, A., Kini, A., Kürnsteiner, P., Raabe, D., & Jägle, E. (2020). Steels in additive manufacturing: A review of their microstructure and properties. *Materials Science And Engineering: A*, *772*, 138633. https://doi.org/10.1016/j.msea.2019.138633

Bhukya, R., Rao, C., & Rao, G. (2014). Evaluation and comparison of Machinability characteristics of Maraging Steel and AISI 304 Steels. *5 Th International & 26Th All India Manufacturing Technology, Design And Research Conference (AIMTDR 2014)*, *473*, 1-7.

Bhushan, B. (2003). Adhesion and stiction: Mechanisms, measurement techniques, and methods for reduction. *Journal Of Vacuum Science & Technology B: Microelectronics And Nanometer Structures*, *21*(6), 2262.

Börder C. (2005). *Análise do coeficiente de atrito no ensaio de anel para o forjamento a quente*, (M.Sc. Thesis). Escola Politécnica da Universidade de São Paulo.

Casati, R., Lemke, J., Tuissi, A., & Vedani, M. (2016). Aging Behaviour and Mechanical Performance of 18-Ni 300 Steel Processed by Selective Laser Melting. *Metals*, *6*(9), 218.

Cristino V. (2007). *Experimental Assessment of Analytical Solutions for Orthogonal Metal Cutting*, (D.Sc. Thesis). Instituto Superior Técnico.

Garmong, G., Paton, N., Chesnutt, J., & Nevarez, L. (1977). An evaluation of the ring test for strain-rate-sensitive materials. *Metallurgical Transactions A*, *8*(12), 2026-2027.

Lohmann, I., Sarvezuk, P., Ferreira, R., Ivashita, F., Da Cas Viegas, A., de Andrade, A., & Paesano, A. (2019). Maraging-300: a structural and hyperfine study of steel aging. *Hyperfine Interactions*, *240*(1).

Male, A. (1965). Variations in friction coefficients of Metals during Compressive Deformation. *Journal Of The Institute Of Metals*, *94*, 121-125.

Opaliński, M., Mazuro, P., Klasik, A. and Rostek, E. (2016). Tribological Examination of Different Steel Materials after Special Heat Treatment and Salt Bath Nitriding. *Archives of Metallurgy and Materials*, *61*(4), 1881-1888.

Prashanth K.G., Eckert J. (2017). Formation of metastable cellular microstructures in selective laser melted alloys. *Journal of Alloys and Compounds*, *707*, 27-34.

Shahriari, D., Sadeghi, M., Ebrahimi, G., & Kim, K. (2011). Effects of lubricant and temperature on friction coefficient during hot forging of Nimonic 115 superalloy. *Metallic Materials*, *49*(05), 375-383.

Sun, K., Peng, W., Wei, B., Yang, L. and Fang, L. (2020). Friction and Wear Characteristics of 18Ni(300) Maraging Steel under High-Speed Dry Sliding Conditions. *Materials 2020*, *13*(7), 1485-1495.

Turk, C., Zunko, H., Aumayr, C., Leitner, H., & Kapp, M. (2019). Advances in Maraging Steels for Additive Manufacturing. *BHM Berg- Und Hüttenmännische Monatshefte*, *164*(3), 112-116. https://doi.org/10.1007/s00501-019-0835-z

Yin, S., Chen, C., Yan, X., Feng, X., Jenkins, R., & O'Reilly, P. et al. (2018). The influence of aging temperature and aging time on the mechanical and tribological properties of selective laser melted maraging 18Ni-300 steel. *Additive Manufacturing*, *22*, 592-600. https://doi.org/10.1016/j.addma.2018.06.005